

NRC Publications Archive Archives des publications du CNRC

Effects of elFiso4G1 mutation on seed oil biosynthesis

Li, Qiang; Shen, Wenyun; Zheng, Qian; Tan, Yifang; Gao, Jie; Shen, Jinxiong; Wei, Yangdou; Kunst, Ljerka; Zou, Jitao

This publication could be one of several versions: author's original, accepted manuscript or the publisher's version. / La version de cette publication peut être l'une des suivantes : la version prépublication de l'auteur, la version acceptée du manuscrit ou la version de l'éditeur.

For the publisher's version, please access the DOI link below./ Pour consulter la version de l'éditeur, utilisez le lien DOI ci-dessous.

Publisher's version / Version de l'éditeur:

https://doi.org/10.1111/tpj.13522 The Plant Journal, 90, 5, pp. 966-978, 2017-02-28

NRC Publications Record / Notice d'Archives des publications de CNRC:

https://nrc-publications.canada.ca/eng/view/object/?id=c9b31e4f-0ca2-49fa-8357-9d0b3fc10f08 https://publications-cnrc.canada.ca/fra/voir/objet/?id=c9b31e4f-0ca2-49fa-8357-9d0b3fc10f08

Access and use of this website and the material on it are subject to the Terms and Conditions set forth at <u>https://nrc-publications.canada.ca/eng/copyright</u> READ THESE TERMS AND CONDITIONS CAREFULLY BEFORE USING THIS WEBSITE.

L'accès à ce site Web et l'utilisation de son contenu sont assujettis aux conditions présentées dans le site https://publications-cnrc.canada.ca/fra/droits LISEZ CES CONDITIONS ATTENTIVEMENT AVANT D'UTILISER CE SITE WEB.

Questions? Contact the NRC Publications Archive team at PublicationsArchive-ArchivesPublications@nrc-cnrc.gc.ca. If you wish to email the authors directly, please see the first page of the publication for their contact information.

Vous avez des questions? Nous pouvons vous aider. Pour communiquer directement avec un auteur, consultez la première page de la revue dans laquelle son article a été publié afin de trouver ses coordonnées. Si vous n'arrivez pas à les repérer, communiquez avec nous à PublicationsArchive-ArchivesPublications@nrc-cnrc.gc.ca.





Received Date : 04-Nov-2016 Revised Date : 01-Feb-2017 Accepted Date : 22-Feb-2017 Article type : Original Article

Effects of eIFiso4G1 mutation on seed oil biosynthesis

Qiang Li^{a,c}, Wenyun Shen^a, Qian Zheng^a, Yifang Tan^a, Jie Gao^d, Jinxiong Shen^d, Yangdou Wei^b, Ljerka Kunst^e, Jitao Zou^a

^aNational Research Council Canada, 110 Gymnasium Place, Saskatoon, Saskatchewan, Canada S7N 0W9; ^bDepartment of Biology, University of Saskatchewan, 112 Science Place, Saskatoon, Saskatchewan, Canada S7N 5E2; ^cDepartment of Plant Science, University of Saskatchewan, 51 Campus Drive, Saskatoon, Saskatchewan, Canada S7N 5A8; ^dNational Key Laboratory of Crop Genetic Improvement, Huazhong Agricultural University, No. 1, Shizi Shan Street, Wuhan, Hubei 430070, China; ^eDepartment of Botany, University of British Columbia, Vancouver, British Columbia, Canada V6T 1Z4

Corresponding author details: Jitao Zou, National Research Council Canada, 110 Gymnasium Place, Saskatoon, Saskatchewan S7N 0W9. Phone 306-975-5583; Fax 306-975-4833; Email: Jitao.Zou@nrc-cnrc.gc.ca

This article has been accepted for publication and undergone full peer review but has not been through the copyediting, typesetting, pagination and proofreading process, which may lead to differences between this version and the Version of Record. Please cite this article as doi: 10.1111/tpj.13522

Running title: Roles of eIFiso4G1 in fatty acid synthesis

Key words: *Arabidopsis thaliana*; fatty acid metabolism; acetyl-CoA carboxylase; mapbased cloning; metabolic interaction; gene expression.

Summary

Fatty acid biosynthesis is a primary metabolic pathway that occurs in plastids, whereas the formation of glycerolipid molecules for the majority of cellular membrane systems and the deposition of storage lipid in seeds takes place in the cytosolic compartment. In this report, we present a study of an Arabidopsis mutant, ar21, with a novel seed fatty acid phenotype showing a higher content of eicosanoic acid (20:1) and oleic acid (18:1) and a reduced level of α -linolenic acid (18:3). A combination of map-based cloning and whole genome sequencing identified the genetic basis underlying the fatty acid phenotype as a lesion in the plant-specific eukaryotic translation initiation factor eIFiso4G1. Transcriptome analysis on developing seeds revealed a reduced level of plastid-encoded genes. Specifically, decreases in both transcript and protein levels of an enzyme involved in lipid biosynthesis, the β -subunit of the plastidic heteromeric acetyl-CoA carboxylase (htACCase) encoded by *accD*, were evident in the mutant. Biochemical assays showed that the developing seeds of the mutant possessed a decreased htACCase activity in the plastid but an elevated activity of homomeric acetyl-CoA carboxylase (hmACCase). These results suggested that the increased 20:1 was attributable at least in part to the enhanced cytosolic hmACCase activity. We also detected a significant repression of FATTY ACID DESATURASE 3 (FAD3) during seed development, which correlated with a decreased 18:3 level in seed oil. Together, our study on a mutant of eIFiso4G1 uncovered multifaceted interactions between the cytosolic and plastidic compartments in seed lipid biosynthesis that impact major seed oil traits.

The fatty acid composition of triacylglycerol (TAG) is an important attribute of seed oil both for food and industrial feed stock uses. The deposition of TAG in seeds depends on close metabolic cooperation between the plastidic and cytosolic compartments. Fatty acid precursors of up to 18-carbon are synthesized in plastids, and subsequently mobilized to the cytosolic compartment in the form of acyl-CoAs. The acyl-CoAs are then assembled onto glycerol backbones to form TAG through the Kennedy pathway (Browse and Somerville, 1991; Ohlrogge and Browse, 1995; Bates and Browse, 2011). In species producing fatty acids with chain lengths exceeding 18-carbons, a portion of fatty acid moieties of the cytosolic acyl-CoA pool are further elongated before being incorporated into TAG (Fehling et al., 1990; Felhing and Mukherjee, 1991; Kunst and Underhill, 1992; Bates et al., 2009; Bates and Browse, 2012). Both fatty acid synthesis in plastids and fatty acid elongation in the cytosol require malonyl-CoA to provide the 2-carbon unit for extension of the fatty acid chain. The provision of malonyl-CoA is mediated by acetyl-CoA carboxylase (ACCase) (Thelen et al., 2001; Thelen and Ohlrogge, 2002; Nikolau et al., 2003; Sasaki and Nagano, 2004).

Two types of ACCase are present in plants: a heteromeric prokaryotic-type complex (htACCase) localized in the plastid and a eukaryotic-type homomeric ACCase (hmACCase) typically present in the cytosol. The htACCase has four subunits: biotin carboxylase carrier protein (BCCP), biotin carboxylase (BC), and the α - and β -subunits of carboxyltransferase (CT) (Shintani et al., 1997; Ke et al., 2000; Li et al., 2010). Plastid ACCase activity is tightly regulated and considered a bottleneck for the overall rate of fatty acid biosynthesis (Page et al., 1994; Roesler et al., 1997). Transcripts of the plastidic htACCase subunits, BC, BCCP1, α -CT, and β -CT, display a constant molar ratio, despite being encoded by two different genomes (Ke et al., 2000; Li et al., 2010). Neither antisense-expression nor over-expression of the BC subunit significantly affected the overall ACCase activity (Shintani et al., 1997).

However, over-expression of the β -CT subunit resulted in an increased protein level of these nuclear-encoded subunits (Madoka et al., 2002), although no apparent effect was detectable at the transcript level.

The hmACCase is a large homomeric protein, in which the four functional subunits equivalent to the plastidic isoforms are integrated into domains of a single polypeptide (Ohlrogge and Jaworski 1997; Sasaki and Nagano, 2004). In Arabidopsis, there are two hmACCases, ACC1 in the cytosol and ACC2 in the plastid (Sasaki and Nagano, 2004). In Arabidopsis, malonyl-CoA in the cytosolic compartment is generated exclusively by ACC1, which has an essential role in the synthesis of TAG and very long chain fatty acids (VLCFAs) such as 20:1 (Agrawal et al., 1984; Roesler et al., 1996; Bao et al., 1998, Baud et al., 2003, Lü et al., 2011, Amid et al., 2012). Recent progresses also suggest a functional significance of plastidic ACC2, which, despite being expressed at a very low level, was able to supply plastidial malonyl-CoA under conditions where chloroplast genome transcription is compromised (Babiychuk et al., 2011).

It has now been established that a significant portion of fatty acids produced in the plastids of developing seeds is first incorporated into phosphatidylcholine (PC) (Bates et al., 2009; Bates and Browse, 2011). Active fatty acyl exchange between PC and the acyl-CoA pool ensues, and vigorous interconversion between PC and diacylglycerol (DAG) provides another route for the eventual incorporation of polyunsaturated and unusual fatty acids into TAG (Lu et al., 2009; Zheng et al., 2012). A critical factor determining TAG fatty acid composition in the seeds is the FATTY ACID DESATURASE3 (FAD3), which catalyzes the conversion of 18:2 to 18:3 on PC (Browse et al., 1993, O'Neill et al., 2011). Coinciding with seed oil deposition, the *FAD3* gene in Arabidopsis is strongly upregulated during the late phase of seed development, and this developmental regulation was recently shown to be modulated by bZIP67 (Mendes et al., 2013).

The coordination between the cytosol and chloroplast compartments for lipid synthesis in vegetative tissues has been extensively studied (Johnson and Williams, 1989; Wallis and Browse, 2002, Li et al., 2015). How such intracellular compartmental coordination influences storage lipid deposition in seeds is also a subject of considerable importance. During a genetic screen, we isolated an Arabidopsis mutant, ar21, which has a premature stop codon mutation in *elFiso4G1*, a plant-specific eukaryotic translation initiation factor isoform previously implicated in regulating chloroplast functions. We show that the altered metabolic coordination between plastid and the cytosol in lipid synthesis was the major cause for seed fatty acid compositional changes in ar21. We also detected a reduced expression of *FAD3*, which resulted in a reduced 18:3 in the seed oil of ar21.

Results

Seeds of ar21 mutant have altered fatty acid composition

In a genetic screen for altered seed fatty acid composition in Arabidopsis, the *ar21* mutant was identified as having a marked decrease in 18:3 and a concomitant increase of 18:1 and 20:1 fatty acids, resulting in a significant decrease in the 18:3/20:1 ratio (Figure 1). These changes were only observed in seeds of *ar21* plants and there was no discernible difference in the fatty acid composition of leaf tissues (Figure S1). To determine the genetic basis of the *ar21* mutation, the *ar21* mutant was crossed to Columbia-0 (Col-0) wild type. F1 plants were grown and allowed to self-pollinate. Of the 565 F2 plants analyzed, 125 showed fatty acid changes similar to that of the original *ar21* seeds. The remaining 440 had fatty acid composition similar to wild type. This pattern of segregation is a good fit to the hypothesized 3:1 ratio (χ^2 =0.114; P > 0.05), indicating that *ar21* is a single recessive mutation. The mutant was further back crossed twice with wild type to provide a more uniform genetic background for subsequent analysis.

Fatty acid changes in developing seeds

To characterize fatty acid changes during seed development, we harvested developing seeds at 5, 7, 9, 11, 13, 15 and 17 DAF (days after flowering). Up to 9 DAF, no differences were detected between wild type and *ar21* in their overall fatty acid profiles (Figure 2). With the onset of TAG deposition (Baud et al., 2002) at 9 DAF, the proportion of 18:1 decreased drastically in wild type but less so in *ar21* (Figure 2a). Both wild type and *ar21* experienced a decrease in 18:3 from 7 DAF to 9 DAF, followed by a rapid increase from 9 DAF to 11 DAF. The level of 18:3 continued to surge in wild type after 11 DAF, whereas in *ar21* mutant it ceased to increase at 13 DAF (Figure 2b). The very long chain fatty acid 20:1 accumulated progressively in both genotypes during later stages of seed development, but from 11 DAF onwards, the amount was consistently higher in *ar21* when compared to wild type (Figure 2c). The total fatty acid content was comparable between wild type and *ar21* throughout seed development and in mature seeds (Figure 2d).

The most stable and dramatic fatty acid changes were observed at 13 DAF. We thus separated different glycerolipid classes and analyzed their respective fatty acid compositions at this particular developmental stage. As shown in Table 1, both phospholipids and neutral lipids displayed similar trends in fatty acid compositional changes, *i.e.*, the levels of 20:1, 18:1 and 18:2 were increased while 18:3 was reduced. We also detected a marked increase of 18:1 in PC, in free fatty acids (FFA) and in TAG. The increase of 18:1 in DAG was marginal and statistically insignificant. Hence, the observed alterations in lipid metabolism in *ar21* were not restricted to TAG biosynthesis.

Molecular identification of the *ar21* as a mutation in *eIFiso4G1*

To identify the genetic lesion underlying the *ar21* fatty acid phenotype, a F2 population from a cross between *ar21* (Col-0) and the *Landsberg erecta* (Ler-0) ecotype was generated. 38 mutants from the F2 population were scored with 20 simple sequence length

polymorphism (SSLP) markers (Jander, 2002) covering the Arabidopsis genome. This allowed us to map the *AR21* gene to chromosome 5. 165 mutant lines were then surveyed with 9 markers on chromosome 5, through which the *AR21* gene was found to be tightly linked to MTH12 and JV65.66, spanning a region of 2000 kilo base pairs on chromosome 5 (Figure 3a).

Whole genome sequencing was then performed with ar21 to pinpoint the causal mutation (Table S1). We identified 899 single nucleotide variants (SNVs) in ar21 when compared to Col-0, among which 133 were found in gene coding regions, including 9 premature-stop mutations (Table S2). One such mutation in At5g57870, previously characterized as encoding eIFiso4G1, was found in the candidate mapping region. This gene was then PCR-amplified from ar21 genomic DNA and the presence of the mutation was verified by sequencing (Figure S2). A single nucleotide change from C to T occurred in the 6th exon of At5g57870, resulting in a premature stop codon (CAA to TAA) (Figure 3a). The At5g57870 gene encodes the plant-specific eukaryotic translation initiation factor 4G (eIF4G) isoform 1 (eIFiso4G1) and a T-DNA insertion mutant of this gene was previously named i4g1 (Lellis et al., 2010).

To verify the causal relationship of the mutation and the seed fatty acid phenotype of ar21, three approaches were taken. First, we conducted mutant-phenotype co-segregation analysis. Genomic DNA was extracted from 107 individual lines from the ar21 x Col-0 F2 population and used for PCR-amplification of the At5g57870 region encompassing the point mutation (Table S3). Ten lines from each genotype (homozygous, ar21/ar21; heterozygous, ar21/AR21; wild type, AR21/AR21) were randomly selected for seed fatty acid analysis. Results confirmed that plants with a homozygous mutation in At5g57870 (ar21/ar21) showed fatty acid changes similar to those of ar21 (Figure S3a). Individual lines were also plotted to show a distribution of fatty acid changes consistent with genotyping data (Figure S3b and

S3c). Second, a T-DNA insertion mutant of the At5g57870 gene, i4g1 (Salk_098730c), was obtained from the ABRC, and its homozygosity was confirmed by PCR (Figure 3b and 3c). A substantial reduction in the transcript level of the At5g57870 gene in comparison to wild type was found in both ar21 and i4g1 mutants (Figure 3d). Seeds of i4g1 showed similar changes in fatty acid profile as ar21 seeds (Figure 3e). Third, genomic fragments of At5g57870 including its promoter region and coding region were amplified from the Col-0 and inserted into the binary vector pMDC123 for genetic transformation of ar21. Transgenic ar21 lines harboring wild type At5g57870 allele showed a restored fatty acid composition similar to wild type seeds (Figure 3e). These results conclusively show that the mutation in At5g57870 was the genetics basis of the ar21 seed fatty acid phenotype.

Gene expression changes in developing seeds of *ar21* and *i4g1*

A previous study with the T-DNA mutant i4g1 reported no developmental or growth phenotype at the seedling stage (Lellis et al., 2010). To investigate the effect of ar21 and i4g1mutations on lipid metabolism in seeds, we performed RNA sequencing (RNAseq) with developing seeds at 13DAF, a stage where the greatest differences in lipid profiles between the wild type and the mutant were observed. To ensure reliability of the RNAseq data, we compared both ar21 and i4g1 with wild type seeds of similar developmental stage, and considered genes differentially regulated only if they displayed at least 1.5 fold changes (FDR < 0.05) in both mutant lines. In total, 277 genes were found to be down-regulated, and 484 genes were up-regulated in the mutant seeds (Data S1). The eIFiso4G1 was previously shown to be localized in the nucleus and the cytoplasm (Koroleva et al., 2004). However, a striking feature that emerged from our RNAseq analysis was that transcripts of genes encoded by the plastidic genome were markedly down-regulated. In ar21 and i4g1, 23 out of the 82 plastid genes displayed transcript levels that were significantly reduced (Fold Change

> 1.5 and FDR < 0.05), while none was found to be up-regulated (Data S2). The down-regulated genes included those involved in photosynthesis (*ATPI*, *NDH*s, *PSA*s and *PSB*s) and ribosomal protein synthesis (*RPL20*, *RPL33*, *RPS11*, *RPS18*, *RPS2*). Other genes such as *CLPP1* and *RBCL* were also repressed. Significantly, the repression of plastid-encoded ribosomal genes in *ar21* was contrasted by an induction of nucleus-encoded ribosomal components of the same translation apparatus (Data S3).

In light of the lipid phenotype of ar21 and i4g1, we focused on differentially expressed genes pertinent to lipid metabolism. Among those encoded by the plastidic genome, the *accD* gene encoding the β -CT subunit of the htACCase was down-regulated in both ar21 (1.91 fold, FDR < 0.1) and i4g1 (2.61 fold, FDR < 0.05) (Data S4). We conducted qRT-PCR analysis of *accD* gene expression and confirmed a reduced transcript level in both ar21 and i4g1 (Figure S4). Among nuclear encoded genes, 36 lipid metabolism-related genes were differentially expressed (Fold Change > 1.5, FDR < 0.05), of which 16 were upregulated and 20 were down-regulated (Data S4). The up-regulated genes included several with putative functions in fatty acid elongation. Also detected in both ar21 and i4g1 was a major reduction in the transcript level of the endoplasmic reticulum FATTY ACID *DESATURASE3* (*FAD3*) (1.65 fold in *ar21*, FDR < 0.05; 1.61 fold in *i4g1*, FDR < 0.05), which mediates the production of 18:3. This reduction of FAD3 gene expression was readily demonstrable through qRT-PCR in 13 DAF seeds (Figure 4a). We further examined the expression of FAD3 at developing stages from 9 to 15 DAF in siliques. As shown in Figure 4b, transcript levels of FAD3 were slightly lower at 9 DAF and 11 DAF, but repressed pronouncedly at 13 DAF and 15 DAF in *ar21*, which coincided with the reduction of 18:3 level in seeds.

The decrease of 18:3 in TAG originates from DAG generated from a less desaturated PC

TAG synthesis can be accomplished through the sequential addition of fatty acyl groups at the *sn-1*, *sn-2* and *sn-3* positions of a glycerol backbone via the Kennedy pathway (Bates et al., 2009; Bates and Browse, 2011), or through transacylation, where the *sn-2* fatty acyl moieties of PC are transferred to the *sn-3* position of DAG (Lu et al., 2009; Zheng et al., 2011). Specific changes at the three positions of the glycerol backbone may give hints as to which of these two pathways is particularly perturbed in the mutant. We thus performed stereo-specific analysis of TAG in wild type and *ar21* seeds. This revealed an increase of 18:1 and 18:2 and a marked decrease of 18:3 at the *sn-2* position of TAG in the mutant seeds (Figure 5a). At the *sn-1,3* positions, 18:3 was decreased as well, but to a lesser degree (Figure 5b). Consistent with previous stereo-specific studies (Zou et al., 1999), the very long chain 20:1 fatty acid was predominately found at the *sn-1,3* position (Figure 5b). Our results indicated that the decreased 18:3 in TAG can largely be ascribed to changes at the *sn-2* position, suggesting that DAG was drawn from a less desaturated PC in the mutant seeds.

Lipidomics analysis confirmed this supposition. The proportion of TAG (18:3) (18:3containing TAG) was significantly decreased in *ar21* (Figure 6a). Potential precursors of 18:3-containing TAGs, including PC (36:6) (Figure 6b) and phosphatidic acid (PA) (36:6) (Figure 6c), were reduced. In addition, 18:3-containing lipids such as phosphatidylethanolamine (PE) (36:6), monogalactosyldiacylglycerol (MGDG) (36:6) and digalactosyldiacylglycerol (DGDG) (36:6) were all decreased in *ar21* mutant when compared to wild type (Data S5). On the other hand, analysis of the 20:1 containing DAG species revealed a reduced amount of 38:4-DAG (20:1/18:3) and an increase of 38:2-DAG (20:1/18:1) (Figure 6d).

Cytosolic and plastdic ACCase activities were readjusted in *ar21*

Plastidic ACCase not only mediates the first committed step but also is the regulatory bottleneck of fatty acid production (Page et al., 1994; Roesler et al., 1997; Sasaki and Nagano, 2004). In Arabidopsis, it is the htACCase that is primarily responsible for malonyl-CoA provision in plastids (Page et al., 1994; Sasaki and Nagano, 2004). To investigate if the *accD* transcript reduction in *ar21* was reflected at the level of its encoded protein, β -CT, we performed western blot analysis on subunits of the htACCase. As shown in Figure 7, there was a clear reduction in β -CT (55kDa) in *ar21* and *i4g1*. We also detected a decreased level of another subunit of the htACCase, BCCP2 (25 kDa) (Figure 7), despite the apparent lack of reduction in the *BCCP2* transcript. These results suggested a role for posttranscriptional regulation in htACCases. Interestingly, we also found that the protein levels of hmACCase (ACC1 and ACC2 with similar molecular weight) were elevated when compared to wild type (Figure 7d), even though their transcript levels appeared slightly lower (Data S4 and Figure S4).

We then examined ACCase activity. Repeated assays showed that the overall ACCase activity in ar21 was lower (3.7 nmol/min/g F.W.) than that of wild type (4.2 nmol/min/g F.W.) (Figure 7e). To assess the specific contribution of the htACCase, fenoxyprop-P-ethyl, a herbicide that specifically inhibits hmACCase (Konishi and Sasaki, 1994; Baud et al., 2004; Oikawa et al., 2006), was included in our enzyme assay. As shown in Figure 7e, the overall ACCase activity in the presence of fenoxyprop-P-ethyl was substantially lower in ar21 (1.9 nmol/min/g F.W.) when compared to that of wild type (3.4 nmol/min/g F.W.); the activity of hmACCase was at 1.7 nmol/min/g F.W. in ar21, and 0.86 nmol/min/g F.W in the wild type. The percentage of htACCase activity was 79.6% and the proportion of hmACCase was 20.4% in wild type developing seeds, which was in line with previous studies (Roesler et al., 1996; Nikolau et al., 2003). In ar21, the proportion of htACCase was reduced to 52.3% of the

total cellular ACCase activity while that of the hmACCase was increased to 47.7% of the total. These biochemical results were consistent with observed protein level changes and suggested that the reduced input of htACCase is compensated in part by a higher hmACCase activity.

Functional redundancy of *eIFiso4G1* and *eIFiso4G2* in seed lipid synthesis

The Arabidopsis genome encodes two plant-specific eIFiso4G translation initiation factors, eIFiso4G1 and eIFiso4G2 (Lellis et al., 2010). The seed fatty acid phenotype was only observed in *eIFiso4G1* null mutants (ar21 and i4g1) (Figure 1 and Figure 3), while loss of *eIFiso4G2* (i4g2; Salk_076633c) had no effect on seed fatty acid composition (Figure S5). The observed changes in lipid composition in the ar21 and i4g1 are stable, but fairly subtle. We thus generated *eIFiso4G1* and *eIFiso4G2* double mutants. Simultaneous deletion of both genes resulted in severe developmental phenotypes that included retarded growth, pale green leaves and shorter siliques (Figure S6). The pleiotropic effect of the *eIFiso4G1* and *eIFiso4G2* double mutation rendered a direct comparison of seed oil composition phenotypes difficult. Nonetheless, the double mutant (i4g1/i4g2) showed a similar trend of changes in seed fatty acid profile, and the extent of the changes was notably heightened when compared to the single mutants (Figure S7). Since single mutants of *eIFiso4G1* (ar21 and i4g1), but not of *eIFiso4G2* (i4g2), exhibited an apparent lipid phenotype in seeds, we concluded that, while *eIFiso4G2* (i4g2), exhibited an apparent lipid phenotype in seeds, we concluded that, while *eIFiso4G2* could partially compensate for the deficiency of *eIFiso4G1*, it was *eIFiso4G1* that played a more prominent role in fatty acid metabolism in seeds.

Discussion

In this study, we characterized an Arabidopsis EMS mutant, which has a novel seed fatty acid phenotype showing increased 20:1 and decreased 18:3. The genetic lesion underlying the altered seed fatty acid composition phenotype was allelic to the previously reported T-DNA mutant i4g1 (Lellis et al., 2010). Plant eIF4G, as in mammals and yeast (Gallie et al., 2001; Mayberry et al., 2011), functions in ribosome attachment and enhancement of the efficiency of mRNA translation in the cytosol. The eIFiso4G proteins, on

the other hand, are plant-specific. It has been proposed that the two eIFiso4G isoforms have distinct substrate preferences for certain mRNAs (Mayberry et al., 2011). However, it remains unclear as to what specific subsets of mRNAs each prefers. Because no developmental and growth phenotypes were apparent in the single mutants, it was also unknown which particular biological processes the two eIFiso4Gs are involved in (Lellis et al., 2010). This study revealed a novel fatty acid phenotype that was only observed in *eIFiso4G1* loss-of-function alleles (*ar21* and *i4g1*) in seeds (Figure 1, Figure 3 and Figure S7), while a deletion of *eIFiso4G2* (*i4g2; Salk_076633c*) had no effect on fatty acid composition (Figure S5 and Figure S7).

A recent study showed that loss of both *eIFiso4G1* and *eIFiso4G2* resulted in higher transcript accumulation of the *NON-PHOTOCHEMICAL QUENCHING 1(NPQ1)* gene (Chen et al., 2014), which encodes violaxanthin de-epoxidase (VDE), a key enzyme for non-photochemical-quenching in chloroplasts. We employed RNAseq to determine which genes had expression profiles that were affected in developing seeds of the two allelic mutants of *eIFiso4G1*, *ar21* and *i4g1*. In the mutant transcriptome, a large set of genes encoded by the plastidic genome displaying reduced transcript levels in developing seed. Significantly, there were contrasting modes of expression changes in nuclear-encoded genes involved in the same biological process. For example, plastid genome genes encoding plastidic ribosomal components were broadly repressed, whereas nuclear encoded components of the chloroplast translational apparatus were mostly induced (Data S3). Such a striking pattern of plastidic and nuclear-encoded gene expression suggests a compensatory response from interacting partners encoded in the nuclear genome.

It is significant that accD, the only gene in lipid metabolism encoded by the plastid genome, was down-regulated in ar21 and i4g1 (Data S4 and Figure S4). The reliability of reduced expression in accD was underscored by the fact that all transcripts of the

polycistronic *accD* operon (Madoka et al., 2002), including *YCF4*, *YCF10* and *PETA*, were expressed at reduced levels as well (Data S2). The *accD* gene encodes a β -subunit of the heteromeric acetyl-CoA carboxylase (htACCase) which catalyzes the first committed step for fatty acid biosynthesis in plastids. These results suggest that lipid metabolism is affected due to compromised plastid gene transcription and/or maintenance of transcript level, particularly *accD*, in the mutant. The negative impact on *accD* transcript level extended to the protein level of the β -CT subunit of the htACCase. Another subunit of the htACCase, BCCP2 was also detected at a decreased protein level. Given that a strict stoichiometric production is required for the assembly of htACCase (Roesler et al., 1996; Thelen et al., 2001; Thelen and Ohlrogge, 2002, Li et al., 2010), the decreased BCCP2 was likely caused by the reduction in β -CT.

Significantly, hmACCase (ACC1 and ACC2) were detected at an increased level. Due to their extremely similar sizes (ACC1, 251 kD; ACC1, 262 kD), it was not possible to accurately assess the specific contributions of each of the two hmACCase isoforms through western blotting. However, other studies have reported that ACC1 accounted for the majority of hmACCase expression, whereas the *ACC2* gene was transcribed at less than 1% of the level of *ACC1* (Roesler et al., 1996; Nikolau et al., 2003). Considering the low expression of *ACC2*, the contribution from ACC2 is likely to be small. Our ACCase activity assays showed that while the htACCase activity was reduced, the total ACCase activity in *ar21* was only slightly lower than that of the wild type. It can be concluded that the steady cellular ACCase activity in *ar21* could be attributed to a higher hmACCase activity. Since ACC1 is responsible for generating malonyl-CoA required for fatty acid elongation in the cytosol (Baud et al., 2003; Lü et al., 2011), we conjecture that the enhanced cytosolic hmACCase activity was the primary cause of higher very long chain fatty acid (20:1) production in *ar21* seeds.

Given that the plastidic htACCase activity, considered a key bottleneck of seed oil biosynthesis, was reduced, it was puzzling that there was no detectable difference in the total fatty acid content of the mutant seeds. It is possible that the reduction of ACCase activity did not reach a level that negatively impacts oil content. Alternatively, malonate produced by the cytosolic ACCase (Roughan et al., 1979) could cross the chloroplast envelope and contributed to malonyl-CoA for fatty acid synthesis in the chloroplast. A caveat of this supposition, however, is that malonate is a poor substrate for fatty acid synthesis using isolated chloroplasts (Roughan et al., 1979). It has been demonstrated that ACC2 is able to supply plastidic malonyl-CoA in the *bsm* mutant, which is deficient in plastidic transcription (Babiychuk et al., 2011). Therefore, we cannot rule out the possibility that ACC2 supplemented plastidic ACCase activity in *ar21* for fatty acid synthesis.

Arabidopsis seed maturation is accompanied by the deposition of storage oil containing substantial amount of polyunsaturated 18:3 fatty acids. Stereo-specific analysis of TAG in *ar21* revealed a major reduction of 18:3 at the *sn-2* position. Since 18:3 is mainly generated on PC by FAD3, our results suggested that the decreased 18:3 at the *sn-2* position of TAG had its origin from a reduced saturation in PC. Consistent with these metabolite changes, we observed that the *FAD3* transcription was repressed during seed maturation. Hence, another significant lipid metabolism-related change in *ar21* was likely caused by a lowered expression of *FAD3*. A recent report indicated that FAD2 and FAD3 form heterodimers which directly convert 18:1-PC to 18:3-PC without releasing 18:2-PC (Lou et al., 2014). In *ar21*, the level of 18:1 fatty acid during seed maturation was persistently higher (Table 1 and Figure 2). Since the decreased 18:3 was accompanied by an increase in 18:1, the flux from 18:1 to 18:3 via 18:2 was likely slower in *ar21*.

In Arabidopsis, there are three eIF4G proteins, eIF4G (At3g60240), eIFiso4G1 (At5g57870) and eIFiso4G2 (At2g24050) (Lellis et al., 2010). Our results from the eIFiso4G1 and eIFiso4G2 double mutant (i4g1/i4g2) showed that some degree of functional redundancy occurred, but it was eIFiso4G1 that played a more prominent role in the seed fatty acid compositional trait. Although not specifically addressed in this study, eIF4G might also contribute to fatty acid synthesis in the absence of the eIFiso4G3. Furthermore, given the large number of genes with altered expression in the eIFiso4G1 mutant, we cannot rule out the possibility that other factors in addition to those highlighted in our results may also contribute to the lipid phenotype.

Experimental procedures

Plant materials and growth conditions

The *ar21* mutant line in the *Arabidopsis thaliana* Col-0 background was isolated from an ethyl methanesulfonate (EMS) mutagenized population as described (Weigel and Glazebrook, 2006). Briefly, about 15,000 Col-0 seeds were mutagenized with freshly prepared EMS solution for 16 hours. These M₁ seeds were then placed on soil and grown in growth chambers at 22/17°C (day/night temperature) and 16 hours light (~120 μ mol m⁻² s⁻¹) /8 hour dark regime. M₂ plants were grown on soil and mature M₃ seeds were screened by gas chromatography for changes in fatty acid composition.

For harvesting developing seeds, only primary shoots were used and secondary shoots were removed. To harvest seeds at defined developmental stage, individual flowers were tagged on the same day of flowering using colored tape. Siliques from 5, 7, 9, 11, 13, 15 and 17 days after flowering (DAF) were harvested and the seeds were dissected out on dry ice. Pools of seeds were stored at -80°C for further analysis. T-DNA mutant lines i4g1

(Salk_098730c) and *i4g2* (Salk_076633c) were obtained from the ABRC (https://www.arabidopsis.org/abrc/) and confirmed with PCR. Plants were grown in growth chambers as described above.

Genetic analysis and map-based cloning

Homozygous *ar21* mutant was backcrossed with Col-0 twice to reduce the number of background mutations and the backcrossed F2 seeds were used for genetic analysis. For mapbased cloning, the *ar21* mutant was crossed to *Landsberg erecta* (Ler) to generate F2 mapping population. In the F2 population, plants with the same fatty acid phenotype as the *ar21* mutant were selected for DNA extraction and mapping. The *AR21* locus was mapped with molecular markers developed based on the Col/Ler polymorphism databank (Table S4) (Lukowitz, 2000; Jander, 2002).

Fatty acid and lipid analysis

Total fatty acids were extracted from ~10 mg mature seeds and fatty acid composition was determined by gas chromatography (GC) with heptadecanoic acid (17:0) as a quantitative internal standard. For time course studies of total fatty acid accumulation, pools of 20~60 seeds were used. For lipid fraction analysis, about 30 mg of developing seeds (13 DAF) were used. Extraction, separation of lipid classes by thin layer chromatography (TLC) plates and analysis of fatty acyl methyl esters by GC were performed as described previously (Shen et al., 2010; Li et al., 2015). Lipid extraction for lipidomic analysis was performed according to the method of Welti (2007).

Total DNA from leaves of three-week old plants was extracted with DNeasy Plant Mini Kit (Qiagen, https://www.qiagen.com/). A 101 bp library was prepared for deepsequencing using NEBNext DNA Sample Prep Master Mix Set 1 (New England BioLabs, https://www.neb.com) and a Genomic DNA Sample Prep Oligo Only Kit (Illumina, www.illumina.com). Prepared libraries were deep-sequenced using an Illumina Genome Analyzer IIx (Illumina). Whole genome assembly was conducted with CLC genomics workbench v7.5 (Qiagen) with default settings and single nucleotide variants (SNVs) against the TAIR10 reference genome sequence of Col-0 were also generated. SNVs with 100% possibility in the candidate region were further examined to identify the mutation sites (Table S1 and S2).

Vector construction

For complementation of the *ar21* mutant line, genomic DNA including the 5' promoter region and the 3' flanking sequence of the gene was cloned into pDONR/Zeo (Invitrogen, now part of Thermo Fisher Scientific, https://www.thermofisher.com) and subsequently moved into the binary vector pMDC123 via BP and LR reactions. The resulting plasmids were introduced into *Agrobacterium tumefaciens* strain GV3101 (pMP90) and then introduced into *ar21* mutant plants using the floral dipping method (Clough and Bent, 1998). Selection of Arabidopsis transformants with BASTA was successfully carried out using both plate-grown (25 ug/ml) and soil-grown (30 mg/L) seedlings.

RNA sequencing and data analysis

Total RNA from developing seeds at 13 DAF were extracted using a Plant RNA Isolation Mini Kit (Agilent, https://www.agilent.com/). The yield and RNA purity were determined spectrophotometrically with Nanodrop 1100 (Thermo Fisher Scientific), and the

quality of the RNA was verified by Agilent 2100 Bioanalyzer (Agilent). Purified total RNA was precipitated and resuspended in RNase-free water to a final concentration of 100 ng/µl. Six cDNA libraries were constructed using the TruSeq RNA Sample Preparation Kit v2 (Illumina) with two replicates for ar21, i4g1 and wild type, respectively. Paired-end sequencing was conducted on the Illumina HiSeq2500 (Illumina), generating 101-nucleotide reads, at the National Research Council Canada, ACRD-Saskatoon, Canada. Sequencing adapters were removed and low-quality reads were trimmed using Trimmomatic with default settings (Bolger et al., 2014). The filtered reads were mapped to TAIR10 genome sequence using STAR (Dobin et al., 2012). Transcripts were identified using StringTie (Pertea et al., 2015) and followed by Cuffmerge tool (Trapnell et al., 2012). HTseq-count (Anders et al., 2014) was employed to count the reads spread across the exonic regions of each gene. Differential expression analysis was performed with DEseq2 between mutants and wild type (Love et al., 2014). Normalized counts from DESeq2 were expressed as gene expression levels. Genes with less than 10 reads across six samples were excluded to eliminate the extremely low expressed transcripts. Ribosomal genes were categorized based on Sormani et al. (2011) (Data S3). Lipid metabolism genes were categorized according to the list from Arabidopsis Acyl-Lipid Metabolism database (http://aralip.plantbiology.msu.edu) (Beisson, 2013) (Data S4). Functional annotations of genes were obtained from the Bio-Array Resource for Arabidopsis Functional Genomics database (BAR) (http://bar.utoronto.ca/) using the AGI numbers.

Stereo-specific analysis

TAGs were extracted from 10 mg of mature seeds as described previously (Zou et al., 1999). For stereo-specific analysis, TAGs were digested with 1mg of Pancreatic lipase (Sigma-Aldrich, https://www.sigmaaldrich.com/) in 1ml reaction buffer (1M Tris-HCl

(pH8.0), 0.1 ml of 2.2% CaCl₂, and 0.25 ml of 0.05% bile salts) at 40°C (Christie et al., 2003). The reaction was stopped by the addition of 1ml of ethanol followed by 1ml of 6M HCl after 3 min. Reaction products were separated on silica TLC plates and developed with hexane/diethyl ether/acetic acid (70:30:1, v/v/v). The spot corresponding to 2-MAG (*sn-2* position of TAG) was subjected to transmethylation and GC analysis. The distribution of fatty acyl groups in the 1,3-MAG (*sn-1,3* position of TAG) was calculated using the following formula: *sn-1,3* (mol %) = [3*TAG (mol %) – *sn-2* (mol %)]/2 (Christie et al., 2003).

Real-time quantitative RT-PCR analyses

Total RNA was extracted from the wild-type and mutant lines with the Plant RNeasy Mini kit. The amount of RNA was determined by Nanodrop 1100 (Thermo Fisher Scientific), and its integrity was assessed by gel electrophoresis. For real-time quantitative RT-PCR (real-time qRT-PCR), 1 μ g of total RNA was used for cDNA synthesis with a QuantiTect Reverse Transcription kit (Qiagen). Gene specific primers (Tm, 57°C -63°C) were designed to generate PCR products between 75 and 130 bps. The specificity of all primers was checked with BLASTn searches (BLAST, http://blast.ncbi.nlm.nih.gov/Blast.cgi). *Tubulin 3* (*At5g62700*) was used as an endogenous control for standardization. Real-time qRT-PCR was performed with Power SYBR Green PCR Master Mix (Applied Biosystems, now part of Thermo Fisher Scientific, https://www.thermofisher.com) and amplification was monitored with ABI StepOne Real-time PCR Systems (Applied Biosystem). A standard thermal profile was used for all PCRs: 50°C for 2 minutes; 95°C for 10 minutes, followed by 40 cycles of 95°C for 15 seconds, 57°C for 30 seconds, 72°C for 30 seconds. Data acquisition and analysis were performed using StepOne software 2.0 (Applied Biosystems).

Approximately 30 mg of developing seeds were homogenized in 300µl of sample buffer according to (Martínez-García et al., 1999). Extracts were centrifuged for 10 min at 13,000 rpm and the supernatant was taken for Bradford assays. For western blots, equal quantities of protein (10 ug) were loaded onto a 12% SDS-polyacrylamide gel. The relative molecular weight of ACCase subunits was determined with protein standards covering a 6 kD to 210 kD range. The polyacrylamide gel was blotted to a nitrocellulose filter, and blots were incubated for 2 hours in Tris buffered saline (TBS) containing 5% skim milk. The α -CT, β -CT and BC subunits of htACCase were immunologically detected with antisera that has been described and characterized previously (Madoka et al., 2002; Kahlau et al., 2008). The antibody for the β -CT subunit was derived from rabbits immunized with oligopeptide containing 14 amino acids (NFMFSKGELEYRGE) (ProSci, http://www.prosci-inc.com/). Biotin containing proteins including hmACCase (ACC1 and ACC2), BCCP1, BCCP2 and MCCase were detected with peroxidase-conjugated streptavidin (500mU/ml in TBS, Roche) (Thelen and Ohlrogge, 2002; Baud et al., 2003). ECL regents were used for visualization.

ACCase activity assay

Siliques at 13DAF were collected and immediately ground in 2 volumes (w/v) of extraction buffer (20 mM TES-KOH pH 7.5, 10% (v/v) glycerol, 5 mM EDTA, 2 mM benzamidine, 2 mM PMSF, 1% (v/v) Triton X100) (Thelen and Ohlrogge, 2002). Homogenates were centrifuged for 1 min at 13,000 g. ACCase activity was quantified by measuring the incorporation of ^[14C] NaHCO3 (American Radiolabeled Chemicals, https://www.arc-inc.com/) into the soluble protein fraction (Roesler et al., 1996). 200 µL of reaction medium containing 100 mM Tricine (pH 8.2), 50 mM KCl, 3 mM ATP, 6 mM MgCl₂, 5 mM DTT, 0.5 mM acetyl-CoA, in the presence or absence of 100 mM fenoxaprop-

P-ethyl (an inhibitor of hmACCase), and 10 mM ^[14C]NaHCO3 (1 mCi/mM). The reaction was initiated by the addition of acetyl-CoA at 25 °C for 20 min. Aliquots of the reaction mixture (100 ul) were mixed vigorously with 40 ul of 12 N HCl to stop the reaction. The solution was then dried under N_2 and the acid-stable radioactivity was quantified in a liquid scintillation counter. Duplicate assays without acetyl-CoA were run as controls.

Accession numbers: Genome sequencing data from this article can be found in the Short Read Archive (SRA) at the National Center for Biotechnology Information under accession number SRP082978. RNA sequencing data can be found in the Gene Expression Omnibus (GEO) under the accession GSE86206.

Acknowledgements

We thank Janet Condie and Dustin Cram from National Research Council Canada-Saskatoon for assistance with Illumina sequencing. We thank J. Allan Feurtado, Mark Smith and Patricia Vrinten for critical reading of our manuscript. We also thank Mary Roth and Ruth Welti of the Kansas Lipidomics Research Center for lipidomic analysis. This research was supported in part by the Natural Sciences and Engineering Research Council of Canada (NSERC) Discovery grant RGPIN-327217-06. This is National Research Council Canada Publication #56239. The authors declare no conflict of interest.

Short Supporting Information Legends

The following supplemental materials are available.
Figure S1. Fatty acid composition in leaves of *ar21* and wild type.
Figure S2. Confirmation of the point mutation in *ar21* by Sanger sequencing.
Figure S3. Seed fatty acid analysis with the *ar21* x Col F2 population.

Figure S4. Quantitative RT-PCR (qRT-PCR) analysis of *accD* and *ACC1*.
Figure S5. Fatty acid composition in mature seeds of wild type and *i4g2*.
Figure S6. Growth phenotypes of wild type, *i4g1*, *i4g2* and *i4g1/i4g2* mutants.
Figure S7. Fatty acid composition in seeds and leaves of wild type and mutants.
Table S1. Summary of genome sequencing data from *ar21*.
Table S2. Summary of premature stop mutations detected in *ar21*.
Table S3. Genotyping with the *ar21* x Col F2 population.
Table S4. Primer pairs used in this study.
Data S1. Differentially expressed genes in the developing seeds of *ar21* and *i4g1*.
Data S3. Differentially expressed ribosomal genes in the developing seeds of *ar21* and *i4g1*.
Data S4. Differentially expressed genes pertinent to lipid metabolism in the developing seeds

of *ar21* and *i4g1*.

Data S5. Lipidomics analysis of developing seeds from *ar21* and wild type.

References

- Agrawal, V.P., Lessire, R., Stumpf, P.K. (1984) Biosynthesis of very long chain fatty acids in microsomes from epidermal cells of *Allium porrum* L. Arch Biochem Biophys. 230: 580-589
- Amid, A., Lytovchenko, A., Fernie, A.R., Warren, G., Thorlby, G.J. (2012) The *sensitive to freezing3* mutation of *Arabidopsis thaliana* is a cold-sensitive allele of homomeric acetyl-CoA carboxylase that results in cold-induced cuticle deficiencies. J Exp Bot. 63: 5289-5299

Anders, S., Pyl, P.T., Huber, W. (2014) HTSeq--a Python framework to work with highthroughput sequencing data. Bioinformatics 31: 166-169

- Babiychuk, E., Vandepoele, K., Wissing, J., Garcia-Diaz, M., De Rycke, R., Akbari, H.,
 Joubes, J., Beeckman, T., Jansch, L., Frentzen, M., Van Montagu, M.C.E., Kushnir, S.
 (2011) Plastid gene expression and plant development require a plastidic protein of the
 mitochondrial transcription termination factor family. Proc Natl Acad Sci USA.108: 6674-6679
- Bao, X., Pollard, M., Ohlrogge, J. (1998) The biosynthesis of erucic acid in developing embryos of *Brassica rapa*. Plant Physiol. 118: 183-190
- Bates, P.D., Browse, J. (2011) The pathway of triacylglycerol synthesis through phosphatidylcholine in Arabidopsis produces a bottleneck for the accumulation of unusual fatty acids in transgenic seeds. Plant J. 68: 387-399
- Bates, P.D., Browse, J. (2012) The significance of different diacylgycerol synthesis pathways on plant oil composition and bioengineering. Front Plant Sci. 3:147
- Bates, P.D., Durrett, T.P., Ohlrogge, J.B., Pollard, M. (2009) Analysis of acyl fluxes through multiple pathways of triacylglycerol synthesis in developing soybean embryos. Plant Physiol. 150: 55-72
- Baud, S., Boutin, J-P., Miquel, M., Lepiniec, L., Rochat, C. (2002) An integrated overview of seed development in *Arabidopsis thaliana* ecotype WS. Plant Physiol Biochem. 40: 151-160
- Baud, S., Guyon, V., Kronenberger, J., Wuilleme, S., Miquel, M., Caboche, M., Lepiniec, L.,
 Rochat, C. (2003) Multifunctional acetyl-CoA carboxylase 1 is essential for very long
 chain fatty acid elongation and embryo development in Arabidopsis. Plant J. 33: 75-86

- Baud, S., Bellec, Y., Miquel, M., Bellini, C., Caboche, M., Lepiniec, L., Faure, J.D., Rochat,
 C. (2004) *gurke* and *pasticcino3* mutants affected in embryo development are impaired in acetyl-CoA carboxylase. EMBO Rep. 5(5):515-520
- Beisson, F. (2003) Arabidopsis Genes Involved in Acyl Lipid Metabolism. A 2003 Census of the Candidates, a Study of the Distribution of Expressed Sequence Tags in Organs, and a Web-Based Database. Plant Physiol. 132: 681-697
- Bolger, A.M., Lohse, M., Usadel, B. (2014) Trimmomatic: a flexible trimmer for Illumina sequence data. Bioinformatics 30: 2114-2120
- Browse, J., McConn, M., James, D, Jr., Miquel, M. (1993) Mutants of Arabidopsis deficient in the synthesis of alpha-linolenate. Biochemical and genetic characterization of the endoplasmic reticulum linoleoyl desaturase. J Biol Chem. 268: 16345-16351
- Browse, J., Somerville, C. (1991) Glycerolipid Synthesis: Biochemistry and Regulation. Annu Rev Plant Physiol Plant Mol Biol. 42: 467-506
- Chen, Z., Jolley, B., Caldwell, C., Gallie, D.R. (2014) Eukaryotic translation initiation factor eifiso4g is required to regulate Violaxanthin De-epoxidase expression in Arabidopsis. J Biol Chem. 289: 13926-13936
- Christie, W.W. (2003) Lipid Analysis: Isolation, Separation, Identification, and Structural Analysis of Lipids. Oily Press, Edition 3.Clough SJ, Bent AF (1998) Floral dip: a simplified method for Agrobacterium-mediated transformation of Arabidopsis thaliana.
 Plant J. 16: 735-743
- Clough, S.J., Bent, A.F. (1998) Floral dip: a simplified method for Agrobacterium-mediated transformation of Arabidopsis thaliana. Plant J. 16(6):735-743

- Dobin, A., Davis, C.A., Schlesinger, F., Drenkow, J., Zaleski, C., Jha, S., Batut, P., Chaisson,M., Gingeras, T.R. (2012) STAR: ultrafast universal RNA-seq aligner. Bioinformatics 29: 15-21
- Fehling, E., Mukherjee, K.D. (1991) Acyl-CoA elongase from a higher plant (*Lunaria annua*): metabolic intermediates of very-long-chain acyl-CoA products and substrate specificity. Biochim Biophys Acta. 1082: 239-246
- Fehling, E., Murphy, D.J., Mukherjee, K.D. (1990) Biosynthesis of triacylglycerols containing very long chain monounsaturated acyl moieties in developing seeds. Plant Physiol. 94: 492-498
- Gallie, D.R., Browning, K.S. (2001) eIF4G functionally differs from eifiso4g in promoting internal initiation, cap-independent translation, and translation of structured mRNAs. J Biol Chem. 276: 36951-36960
- Jander, G. (2002) Arabidopsis map-based cloning in the post-genome era. Plant Physiol. 129: 440-450
- Johnson, G., Williams, J.P. (1989) Effect of growth temperature on the biosynthesis of chloroplastic galactosyldiacylglycerol molecular species in *Brassica napus* leaves. Plant Physiol. 91: 924-929
- Kahlau, S., Bock, R. (2008) Plastid transcriptomics and translatomics of tomato fruit development and chloroplast-to-chromoplast differentiation: chromoplast gene expression largely serves the production of a single protein. Plant Cell 20: 856-874
- Ke, J., Wen, T.N., Nikolau, B.J., Wurtele, E.S. (2000) Coordinate Regulation of the Nuclear and Plastidic Genes Coding for the Subunits of the Heteromeric Acetyl-Coenzyme A Carboxylase. Plant Physiol. 122: 1057-1071

- Konishi, T., Sasaki, Y. (1994) Compartmentalization of two forms of acetyl-CoA carboxylase in plants and the origin of their tolerance toward herbicides. Proc Natl Acad Sci U S A. 91(9):3598-3601
- Koroleva, O.A., Tomlinson, M.L., Leader, D., Shaw, P., Doonan, J.H. (2004) Highthroughput protein localization in Arabidopsis using Agrobacterium-mediated transient expression of GFP-ORF fusions. Plant J. 41: 162-174
- Kunst, L., Underhill, E.W. (1992) Fatty acid elongase in developing seeds of *Arabidopsis thaliana*. Plant Physiol Biochem. 30: 425-434
- Lellis, A.D., Allen, M.L., Aertker, A.W., Tran, J.K., Hillis, D.M., Harbin, C.R., Caldwell, C., Gallie, D.R., Browning, K.S. (2010) Deletion of the eIFiso4G subunit of the Arabidopsis eIFiso4F translation initiation complex impairs health and viability. Plant Mol Biol. 74: 249-263
- Li, Q., Zheng, Q., Shen, W., Cram, D., Fowler, D.B., Wei, Y., Zou, J. (2015) Understanding the biochemical basis of temperature-induced lipid pathway adjustments in plants. Plant Cell 27: 86-103
- Li, X., Ilarslan, H., Brachova, L., Qian, H.R., Li, L., Che, P., Wurtele, E.S., Nikolau, B.J.
 (2010) Reverse-genetic analysis of the two biotin-containing subunit genes of the heteromeric acetyl-coenzyme a carboxylase in Arabidopsis indicates a unidirectional functional redundancy. Plant Physiol. 155: 293-314
- Lou, Y., Schwender, J., Shanklin, J. (2014) FAD2 and FAD3 desaturases form heterodimers that facilitate metabolic channeling *in Vivo*. J Biol Chem. 289: 17996-18007
- Love, M.I., Huber, W., Anders, S. (2014) Moderated estimation of fold change and dispersion for RNA-seq data with DESeq2. Genome Biol. 15(12)

- Lu, C., Xin, Z., Ren, Z., Miquel, M., Browse, J. (2009) An enzyme regulating triacylglycerol composition is encoded by the *ROD1* gene of Arabidopsis. Proc Natl Acad Sci USA. 106: 18837-18842
- Lü, S., Zhao, H., Parsons, E.P., Xu, C., Kosma, D.K., Xu, X., Chao, D., Lohrey, G.,
 Bangarusamy, D.K., Wang, G., Bressan, R.A., Jenks, M.A. (2011) The *glossyhead1* allele of ACC1 reveals a principal role for multidomain acetyl-coenzyme A carboxylase in the biosynthesis of cuticular waxes by Arabidopsis. Plant Physiol. 157: 1079-1092
- Lukowitz, W. (2000) Positional Cloning in Arabidopsis. Why it feels good to have a genome initiative working for you. Plant Physiol. 123: 795-806
- Madoka, Y., Tomizawa, K., Mizoi, J., Nishida, I., Nagano, Y., Sasaki, Y. (2002) Chloroplast transformation with modified accD operon increases Acetyl-CoA carboxylase and causes extension of leaf longevity and increase in seed yield in tobacco. Plant Cell Physiol. 43: 1518-1525
- Martínez-García, J.F., Monte, E., Quail, P.H. (1999) A simple, rapid and quantitative method for preparing Arabidopsis protein extracts for immunoblot analysis. Plant J. 20: 251-257
- Mayberry, L.K., Allen, M.L., Nitka, K.R., Campbell, L., Murphy, P.A., Browning, K.S.(2011) Plant cap-binding complexes eukaryotic initiation factors eif4f and eifiso4f:molecular specificity of subunit binding. J Biol Chem. 286: 42566-42574
- Mendes, A., Kelly, A.A., van Erp, H., Shaw, E., Powers, S.J., Kurup, S., Eastmond, P.J.
 (2013) bZIP67 regulates the omega-3 fatty acid content of arabidopsis seed oil by activating *FATTY ACID DESATURASE3*. Plant Cell 25: 3104-3116
- Nikolau, B.J., Ohlrogge, J.B., Wurtele, E.S. (2003) Plant biotin-containing carboxylases. Arch Biochem Biophys. 414: 211-222

O'Neill, C.M., Baker, D., Bennett, G., Clarke, J., Bancroft, I. (2011) Two high linolenic mutants of *Arabidopsis thaliana* contain megabase-scale genome duplications encompassing the FAD3 locus. Plant J. 68: 912-918

Ohlrogge, J., Browse, J. (1995) Lipid Biosynthesis. Plant Cell 7: 957-970

- Ohlrogge, J.B., Jaworski, J.G. (1997) Regulation of fatty acid synthesis. Annu Rev Plant Physiol Plant Mol Biol. 48: 109-136
- Oikawa, A., Nakamura, Y., Ogura, T., Kimura, A., Suzuki, H., Sakurai, N., Shinbo, Y., Shibata, D., Kanaya, S., Ohta, D. (2006) Clarification of pathway-specific inhibition by fourier transform ion cyclotron resonance/mass spectrometry-based metabolic phenotyping studies. Plant Physiol. 142: 398-413
- Page, R.A., Okada, S., Harwood, J.L. (1994) Acetyl-CoA carboxylase exerts strong flux control over lipid synthesis in plants. Biochim Biophys Acta. 1210: 369-372
- Pertea, M., Pertea, G.M., Antonescu, C.M., Chang, T-C., Mendell, J.T., Salzberg, S.L. (2015) StringTie enables improved reconstruction of a transcriptome from RNA-seq reads. Nat Biotechnol. 33: 290-295
- Roesler, K., Savage, L., Shintani, D., Shorrosh, B., Ohlrogge, J. (1996) Co-purification, coimniunoprecipitation, and coordinate expression of acetyl-coenzyme A carboxylase activity, biotin carboxylase, and biotin carboxyl carrier protein of higher plants. Planta 198: 517-525
- Roesler, K., Shintani, D., Savage, L., Boddupalli, S., Ohlrogge, J. (1997) Targeting of the Arabidopsis homomeric acetyl-coenzyme A carboxylase to plastids of rapeseeds. Plant Physiol 113: 75-81

Roughan, P.G., Holland, R., Slack, C.R. (1979) Acetate is the preferred substrate for longchain fatty acid synthesis in isolated spinach chloroplasts. Biochem J. 15;184(3): 565-569.

- Sasaki, Y., Nagano, Y. (2004) Plant acetyl-CoA carboxylase: structure, biosynthesis, regulation, and gene manipulation for plant breeding. Biosci Biotechnol Biochem. 68: 1175-1184
- Shen, W., Li, J.Q., Dauk, M., Huang, Y., Periappuram, C., Wei, Y., Zou, J. (2010) Metabolic and transcriptional responses of glycerolipid pathways to a perturbation of glycerol 3phosphate metabolism in Arabidopsis. J Biol Chem. 285: 22957-22965
- Shintani, D., Roesler, K., Shorrosh, B., Savage, L., Ohlrogge, J. (1997) Antisense expression and overexpression of biotin carboxylase in tobacco leaves. Plant Physiol. 114: 881-886
- Sormani, R., Masclaux-Daubresse, C., Daniel-Vedele, F., Chardon, F. (2011) Transcriptional regulation of ribosome components are determined by stress according to cellular compartments in *Arabidopsis thaliana*. PLoS One 6: e28070
- Thelen, J.J., Mekhedov, S., Ohlrogge, J. (2001) Brassicaceae Express multiple isoforms of biotin carboxyl carrier protein in a tissue-specific manner. Plant Physiol. 125: 2016-2028
- Thelen, J.J., Ohlrogge, J.B. (2002) Both antisense and sense expression of biotin carboxyl carrier protein isoform 2 inactivates the plastid acetyl-coenzyme A carboxylase in *Arabidopsis thaliana*. Plant J. 32: 419-431
- Trapnell, C., Roberts, A., Goff, L., Pertea, G., Kim, D., Kelley, D.R., Pimentel, H., Salzberg,S.L., Rinn, J.L., Pachter, L. (2012) Differential gene and transcript expression analysis ofRNA-seq experiments with TopHat and Cufflinks. Nat Protoc 7: 562-578

Wallis, J.G., Browse, J. (2002) Mutants of Arabidopsis reveal many roles for membrane lipids. Prog Lipid Res. 41: 254-278

- Weigel, D., Glazebrook, J. (2006) EMS mutagenesis of Arabidopsis seed. Cold Spring Harbor Protocols 2006: pdb.prot4621-pdb.prot4621
- Welti, R. (2007) Plant lipidomics: Discerning biological function by profiling plant complex lipids using mass spectrometry. Frontiers in Bioscience 12: 2494-2506
- Zheng, Q., Li, J.Q., Kazachkov, M., Liu, K., Zou, J. (2012) Identification of *Brassica napus* lysophosphatidylcholine acyltransferase genes through yeast functional screening.Phytochemistry 75: 21-31
- Zou, J., Wei, Y., Jako, C., Kumar, A., Selvaraj, G., Taylor, D.C. (1999) The Arabidopsis thaliana TAG1 mutant has a mutation in a diacylglycerol acyltransferase gene. Plant J. 19: 645-653

Table 1 Lipid analysis with *ar21* mutant and wild type (WT) in developing seeds. Seeds were harvested at 13 days after flowering (DAF). Fatty acid compositions in neutral (triacylglycerols, TAG and diacylglycerols, DAG), polar lipids (phosphatidylcholine, PC and phosphatidylethanolamine, PE), free fatty acid (FFA) and total fatty acids (TFA) were analyzed. 16:1 includes *cis* and *trans* 16:1 fatty acid. -, not detected. Values are expressed as means \pm SD (n = 3). Statistical significance was calculated by student t-test. *, p value < 0.05.

		Fatty acid composition (mol%)						
		16:0	16:1	18:0	18:1	18:2	18:3	20:1
TAG								
	WT	9.5±0.4	0.7 ± 0.0	3.5±0.4	14.7±0.2	28.6±1.0	19.4±1.6	18.1±0.6
	ar21	8.7±0.1*	0.6 ± 0.0	3.1±0.1	15.9±0.2*	*31.4±0.3*	*15.3±0.2*	*19.8±0.3*
DAG								
	WT	13.8±1.8	-	5.5±1.1	17.9±0.8	29.1±1.9	17.5±1.3	13.1±1.4
	ar21	14.3±0.7	-	6.7±1.1	18.0±0.4	30.7 ± 1.4	14.8±0.4*	*12.9±0.4
PC								
	WT	14.9±0.3	1.2±0.0	2.5±0.2	9.6±1.8	42.3±1.5	24.5±1.1	3.3±0.6
	ar21	13.6±0.7*	[∗] 1.1±0.0	2.9±0.3*	13.9±1.5*	*46.2±1.3*	[•] 18.9±1.1 [*]	*4.5±0.1*
PE								
	WT	32.0±1.7	-	3.5±1.1	6.2±1.3	32.3±3.3	25.7±2.3	1.4±0.6
	ar21	25.7±1.0*	k_	3.6±1.4	6.0±0.6	40.3±0.5*	^c 23.2±1.0	1.2±0.0
FFA								
	WT	29.2±1.0	-	21.5±0.5	11.8±0.2	12.2±0.1	6.5±0.5	13.6±0.5
	ar21	19.2±0.8*	k_	21.2±3.0	17.8±1.8*	*12.6±1.0	4.5±0.6*	19.9±1.0*
TFA								
	WT	9.3±0.4	0.4 ± 0.0	3.6±0.1	14.6±0.6	29.0±0.1	19.6±0.8	17.6±0.2
	ar21	8.5±0.1*	0.5 ± 0.0	3.2±0.1*	19.2±0.1*	*29.9±0.1*	*15.1±0.3*	*18.5±0.1*

Figure legends

Figure 1. Fatty acid composition in mature seeds of *ar21* mutant and wild type (WT).

16:1 includes *cis* and *trans*-16:1 fatty acid. Values are expressed as means \pm SD (n = 3).

Statistical significance was calculated by Student's t-test. **, p value < 0.01, ***, p value <

0.001.

Figure 2. Fatty acid composition in ar21 mutant and wild type (WT) during seed

maturation. Major fatty acids with significant changes during seed maturation were plotted as following: (a) 18:1 fatty acid; (b) 18:3 fatty acid; (c) 20:1 fatty acid; (d) total fatty acid content per seed. Values are expressed as means \pm SD (n = 3).

Figure 3. Map-based cloning and whole genome sequencing using *ar21* **mutant.** (a) Mapbased cloning and the pre-mature stop mutation identified in At5g57870. BACs, bacterial artificial chromosome. (b) Position of point mutation in *ar21* and T-DNA insertion in *i4g1* mutant. (c) PCR confirmation with T-DNA line. WT, wild type; *i4g1*, T-DNA mutant; *i4g1/*WT, heterozygous line. (d) Relative expression levels of At5g57870 in 13DAF seeds of *ar21* and *i4g1* mutants. (e) Seed fatty acid analysis with wild type, *i4g1* and *ar21c* (complementation line). 16:1 includes *cis* and *trans*-16:1 fatty acid. Data are means \pm SD (*n* = 3). WT, wild type; *, p value < 0.05; **, p value < 0.01, ***, p value < 0.001 (by Student's ttest).

Figure 4. Expression of FAD3 during seed maturation. (a) Validation of FAD3

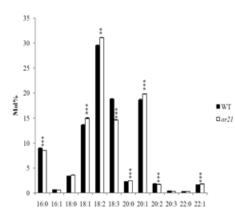
expression. Quantitative RT-PCR (qRT-PCR) was conducted with 13 DAF seeds from *ar21*, *i4g1* and wild type (WT). (b) Relative expression of *FAD3* in *ar21* at 9, 11, 13 and 15DAF. Relative expression of *FAD3* in mutants was presented as fold change against WT. Values are expressed as mean \pm SD (n=3). *, p value < 0.05; ***, p value < 0.001 (by Student's ttest).

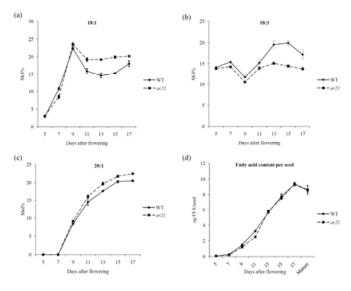
Figure 5. Stereo-specific analysis with TAG from mature seeds of *ar21* and wild type (WT). (a) Lipid composition at the *sn-2* position of TAG (2-MAG) in *ar21* and WT. (b) Lipid composition at the *sn-1,3* positions of TAG (1,3-DAG) in *ar21* and WT. Data are mean \pm SD (n=3). **, p value < 0.01; ***, p value < 0.001 (by Student's t-test).

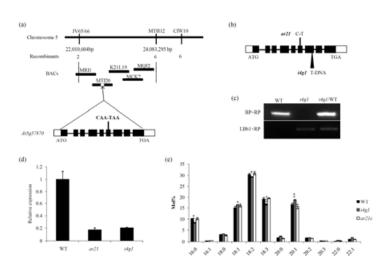
Figure 6. Lipidomics analysis with developing seeds of *ar21* mutant and wild type (WT). Seeds of *ar21* mutant and WT at 13DAF were collected for lipidomics analysis. (a) Proportion of individual lipids in total lipid signal in *ar21* mutant and WT. TAG or DAG species containing particular fatty acyl groups are indicated in brackets. Compositions of molecular species in PC (b), PA(c) and DAG (20:1) (d) were plotted. Data are mean \pm S.D. (n=5). *, p value < 0.05; ***, p value < 0.001 (by Student's t-test).

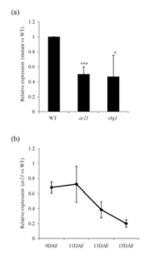
Figure 7. Alterations in plastidic and cytosolic ACCases. (a) Western blot analysis of ACCases in mutants and wild type (WT). Protein expression of htACCase subunits (BCCP1, BCCP2, α-CT, β-CT and BC) and hmACCases (ACC1 and ACC2) in 13DAF developing seeds from *ar21*, *i4g1* and WT. Expression of biotinylated 3-methylcrotonyl CoA carboxylase (MCCase) is used as internal control. Relative expression values of BCCP2 (b), β-CT (c) and hmACCases (d) in *ar21* and *i4g1* mutants were expressed as a ratio of WT by quantitative, densitometric analysis of protein expression from western blots (A) in triplicates. All values were normalized with respect to the intensities of MCCase using ImageJ software. Values are expressed as mean \pm SD of three replicates. (e) ACCase activity measurements. The ACCase activity was assayed using developing siliques (13 DAF) from WT and *ar21* in the presence, or absence, of acetyl-CoA. In order to assess htACCase activity, fenoxaprop-P-ethyl, an inhibitor of the hmACCase was added. Data are expressed as mean \pm SD (n=6). **, p value < 0.01; ***, p value < 0.001 (by Student's t-test).



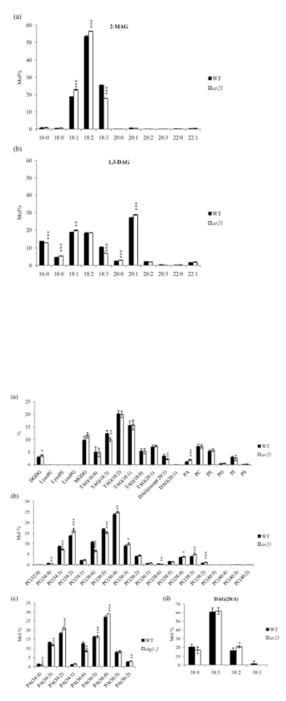












This article is protected by copyright. All rights reserved.



